Published in final edited form as:
Mol Pharmacol. 1994 June ; 45(6): 1101–1111.

A Binding Site Model and Structure-Activity Relationships for the Rat A_3 Adenosine Receptor

PHILIP J. M. VAN GALEN, **ANDREW H. VAN BERGEN**, **CAROLA GALLO-RODRIGUEZ**, **NELI MELMAN**, **MARK E. OLAH**, **AD P. IJZERMAN**, **GARY L. STILES**, and **KENNETH A. JACOBSON**

Molecular Recognition Section, Laboratory of Bioorganic Chemistry, National Institute of Diabetes, Digestive and Kidney Diseases, National Institutes of Health, Bethesda, Maryland 20892 (P.J.M.v.G., A.H.v.B., C.G.-R., N.M., K.A.J.), Departments of Medicine and Pharmacology, Duke University Medical Center, Durham, North Carolina 27710 (M.E.O., G.L.S.), and Division of Medicinal Chemistry, Center for Bio-Pharmaceutical Sciences, Leiden, The Netherlands (A.P.IJ.)

SUMMARY

A novel adenosine receptor, the A_3 receptor, has recently been cloned. We have systematically investigated the hitherto largely unexplored structure-activity relationships (SARs) for binding at A_3 receptors, using ^{125}I-N^6-2-(4-aminophenyl)ethyladenosine as a radioligand and membranes from Chinese hamster ovary cells stably transfected with the rat A_3-cDNA. As is the case for A_1 and A_{2a}, receptors, substitutions at the N^6 and 5′ positions of adenosine, the prototypic agonist ligand, may yield fairly potent compounds. However, the highest affinity and A_3 selectivity is found for N^6,5′-disubstituted compounds, in contrast to A_1 and A_{2a} receptors. Thus, N^6-benzyladenosine-5′-*N*-ethylcarboxamide is highly potent (K_i, 6.8 nM) and moderately selective (13- and 14-fold versus A_1 and A_{2a}). The N^6 region of the A_3 receptor also appears to tolerate hydrophilic substitutions, in sharp contrast to the other subtypes. Potencies of N^6,5′-disubstituted compounds in inhibition of adenylate cyclase via A_3 receptors parallel their high affinity in the binding assay. None of the typical xanthine or nonxanthine (A_1/A_2) antagonists tested show any appreciable affinity for rat A_3 receptors. 1,3-Dialkylxanthines did not antagonize the A_3 agonist-induced inhibition of adenylate cyclase. A His residue in helix 6 that is absent in A_3 receptors but present in A_1/A_2 receptors may be causal in this respect. In a molecular model for the rat A_3 receptor, this mutation, together with an increased bulkiness of residues surrounding the ligand, make antagonist binding unfavorable when compared with a previously developed A_1 receptor model. Second, this A_3 receptor model predicted similarities with A_1 and A_2 receptors in the binding requirements for the ribose moiety and that xanthine-7-ribosides would bind to rat A_3 receptors. This hypothesis was supported experimentally by the moderate affinity (K_i 6 μM) of 7-riboside of 1,3-dibutylxanthine, which appears to be a partial agonist at rat A_3 receptors. The model presented here, which is consistent with the detailed SAR found in this study, may serve to suggest future chemical modification, site-directed mutagenesis, and SAR studies to further define essential characteristics of the ligand-receptor interaction and to develop even more potent and selective A_3 receptor ligands.

Adenosine receptors, belonging to the superfamily of the G protein-coupled receptors, are generally divided into two major subclasses, A_1 and A_2, on the basis of the following: (i) the differential affinities of a number of adenosine receptor agonists and antagonists; (ii) their primary structures; (iii) the second messenger systems to which they couple. Thus, A_2

Send reprint requests to: Kenneth A. Jacobson, Bldg. 8A, Rm. B1A-17, NIDDK, NIH, Bethesda, MD 20892.

receptors (which can be further subdivided into A_{2a} and A_{2b}) stimulate adenylate cyclase, whereas A_1 receptors may couple to a variety of second messenger systems, including inhibition of adenylate cyclase, inhibition or stimulation of phosphoinositol turnover, activation of guanylate cyclase, activation of potassium influx, and inhibition of calcium influx (1, 2). A recent addition to the adenosine receptor family has been the A_3 receptor, which was cloned from rat brain (3) and rat testis (4) and which was first recognized as an adenosine receptor on the basis of its primary structure. In the putative transmembrane domains, it shows 58% identity with the canine A_1 receptor and 57% with the canine A_{2a} receptor. Like the A_1 receptor, it is negatively coupled to adenylate cyclase (3).

The physiological role of the A_3 receptor is mostly unexplored. Its distribution is fairly limited, and it is found primarily in the central nervous system (3), testes (4), heart (3), and the immune system, where it appears to be involved in the modulation of release from mast cells or other cells of mediators of the immediate hypersensitivity reaction (5). Activation of A_3 receptors also appears to cause xanthine-insensitive hypotensive response in pithed rats (44). In terms of therapeutic potential, a principal deficiency of A_1- and A_{2a}-selective agents has been their propensity for side effects, due to the ubiquitous nature of these receptors. However, the limited distribution of A_3 receptors raises hopes that A_3-selective compounds may be more useful as potential therapeutic agents.

Few ligands for this novel receptor have been reported.[1] Some nonselective N^6-substituted adenosine derivatives have been described as agonists for the A_3 receptor, including APNEA (N^6-2-(4-aminophenyl)ethyladenosine), which has been used successfully as a radioligand in its iodinated form (3). Curiously, xanthines (classical A_1 and A_2 antagonists) do not appear to bind to this receptor (3). Because the SAR at A_3 receptors is practically unexplored, we have systematically investigated a wide range of purine and nonpurine agents for affinity in binding to arrive at leads for achieving selectivity. We have integrated these pharmacological findings with insights derived from molecular modeling of A_1 receptors to present a binding site model unique for A_3 receptors.

Materials and Methods

Chemicals

F-12 (Ham's) medium, fetal bovine serum, and penicillin/streptomycin were from Life Technologies, Inc. (Gaithersburg, MD) [^{125}I] APNEA was prepared as described previously (6). Adenosine deaminase (ADA) was from Boehringer Mannheim (Indianapolis, IN). Composition of lysis buffer was as follows: 10 mM Tris, 5 mM EDTA, pH 7.4, at 5 °. 50/10/1 buffer was as follows: 50 mM Tris, 10 mM $MgCl_2$, 1 mM EDTA, pH 8.26, at 5 °. Displaces were from RBI (Natick, MA) except xanthine, inosine, 8-chlorotheophylline (Aldrich, Milwaukee, WI); 1,9-dimethylxanthine, 3,9-dimethylxanthine (Fluka, Ronkonkoma, NY); 3,7-dimethylxanthine, 8-bromoadenosine, adenosine-*N*-oxide, α-D-adenosine, 2′-deoxyadenosine, 3′-deoxyadenosine, 5′-deoxyadenosine, 5′-deoxy-5′-methylthioadenosine, 5′-deoxy-5′-isobutylthioadenosine, S-adenosylmethionine, guanosine, 6-thioguanosine, 6-thiopurine riboside (Sigma); AMP (Boehringer Mannheim); xanthosine, uridine, thymidine, cytidine (Janssen/Spectrum, Gardens, CA). The following compounds were gifts, which are gratefully acknowledged: 1,3-dibutylxanthine, 1,3-dihexylxanthine, 1,3-dibenzylxanthine, 8-cyclohexycaffeine, 7-benzyltheophylline, N^6-dimethyladenosine, 3-deazaadenosine, 7-deazaadenosine, β-L-adenosine, 2′-*O*-methyladenosine, adenine-β-D-arabinofuranoside, xylofuranosyladenosine, β-D-psicofuranosyladenine, 5′-deoxy-5′-

[1]During preparation of this paper, the cloning of the sheep A_3 receptor was reported (Linden *et al.,* Mol. Pharmacol., 1993, 44:524-532). At this receptor, certain xanthine derivatives do bind and act as antagonists, albeit in most cases with diminished affinity relative to A_1 receptors.

aminoadenosine, 5′-carboxamidoadenosine, 2-thio-3-propylxanthine, 1-propyl-8-cyclopentylxanthine (Dr. J. Daly, NIH, Bethesda, MD); N^6-cyclohexylNECA, 9-ethyl-N^6-cyclopentyladenine, N^6-dimethylNECA, N^6-benzyl-N^6-methyladenosine (Dr. R. Olsson, University of South Florida, Tampa, FL); CP 66713 (Dr. R. Sarges, Pfizer, Groton, CT); CGS 15943, (Dr. J. Francis, Ciba-Geigy, Summit, NJ). The syntheses of the following compounds have been described previously: theophylline-7-riboside, 1,3-dipropylxanthine-7-riboside, 1,3-dibutylxanthine-7 riboside (7); imidazo[4,5-*c*]quinolin-4-amine (8); N^6-2-sulfoethyladenosine, N^6-4-sulfophenyladenosine, N^6-3-(4-sulfophenyl)-propyladenosine, N^6-4-(4-sulfophenyl)butyladenosine (9). All other materials were from standard local sources and of the highest grade commercially available.

Synthesis

N^6-Benzyladenosine-N^1-oxide—N^6-Benzyladenosine (25 mg, 70 μmol) and *m*-chloroperbenzoic acid (38 mg, 220 μmol) were dissolved in 1 ml of acetic acid. The solution was stirred at room temperature for 2 days. The solvent was evaporated under a stream of nitrogen, and the residue was dissolved in a minimum of methanol and chromatographed on a silica plate (250 μ) using acetonitrile:water, 4:1 (v/v). The UV-absorbing band at R_F = 0.53 was extracted with methanol to provide 7.3 mg (28% yield). Mass spectrum and ^{1}H-NMR spectrum were consistent with the assigned structure.

Adenosine-5′-*N*-ethyluronamide-N^1-oxide—Adenosine-5′-*N*-ethyluronamide-N^1-oxide was synthesized by a method similar to N^6-benzyladenosine-N^1-oxide. Following recrystallization from hot methanol/ether, the pure product was obtained in 28% yield. Mass spectrum (electron impact, peaks at 324 (m), 308) and ^{1}H-NMR spectrum were consistent with the assigned structure.

N^6-Benzyladenosine-5′-*N*-ethyluronamide—To a solution of NECA (50 mg, 0.162 mmol) in DMF (1 ml) was added benzyl bromide (56 ml, 0.47 mmol), and the solution was stirred for 2 days at 40 ° while protected from moisture. DMF was removed *in vacuo* giving a syrup that crystallized when acetone and ether were added. The solvent was removed by decantation, and the solid was dried and dissolved in methanol (2 ml). K_2CO_3 (10 mg) was added and warmed under reflux overnight. The reaction mixture was cooled, filtered, and evaporated. The product was purified by preparative TLC ($CHCl_3$:MeOH, 13:2) in 42% yield. Melting point, 170–173 °. ^{1}H-NMR (in Me_2SO-d_6) was as follows: δ 1.06 (t, J = 7 Hz, 3H, CH_3), 3.20 (m, 2H, CH_2), 4.13 (t, J = 4Hz, 1H, H-3′), 4.30 (s, 1H, H-4′), 4.62 (m, 1H, H-2′), 4.71 (broad s, 2H, N^6-C$\underline{H}_2$Ph), 5.53 (d, J = 7 Hz, 1H, OH-2′), 5.73 (d, J = 4 Hz, 1H, OH-3′), 5.96 (d, J = 8 Hz, 1H, H-1′), 7.30 (m, 5H, Phenyl), 8.25 (s, 1H, H-2), 8.42 (s, 1H, H-8), 8.55 (broad s, 1H, $N^6\underline{H}$-CH_2Ph), 8.86 (t, J = 5 Hz, 1H, NH-Et). Mass Spectrum (CI-NH_3): *m/z* 399 (MH^+, base).

Inosine-5′-*N*-ethyluronamide (NECI)—2′,3′-*O*-Isopropylideneinosine-5′-uronic acid (20 mg, 62 μmol) (10), 1-[3-(dimethylamino)propyl]-3-ethylcarbodiimide hydrochloride (25 mg, 130 μmol) and *N*-hydroxysuccinimide (13 mg, 112 μmol) were dissolved in a minimum volume of dimethylformamide. Ethylamine (70% in water, 7 μl) was added and after 1 hr of stirring, was cooled to 0 °, and was precipitated with water to give 14 mg (65% yield). The product (10 mg, 29 μmol) was heated in 1 N HCl for 2 hr at 60 °. After cooling and neutralizing with $NaHCO_3$, it was purified twice using reverse phase SepPak cartridges with water as eluant. Lyophilization of the fraction afforded 6.95 mg (78% yield) of an amorphous solid Melting point, 168°C (d). ^{1}H-NMR (in Me_2SO-d_6) was as follows: δ 1.03 (t, J = 7 Hz, 3H, CH_3), 3.17 (m, 2H, CH_2), 4.15 (broad s, 1H, H-3′), 4.30 (s, 1H, H-4′), 4.54 (m, 1H, H-2′), 5.61 (broad s, 1H, OH), 5.68 (broad s, 1H, OH), 5.96 (d, J = 7 Hz, 1H, H-1′), 8.08 (s, 1H, H-2), 8.39 (s, 1H, H-8). Mass spectrum (CI-NH_3): *m/z* 310 (MH^+, base).

Cell culture and membrane preparation

CHO cells stably expressing the rat A_3 receptor (3) were grown in F-12 medium containing 10% fetal bovine serum and penicillin/streptomycin (100 units/ml and 100 μg/ml, respectively) at 37 ° in a 5% CO_2 atmosphere. When cells had reached confluency, they were washed twice with 10 ml of ice-cold lysis buffer. After addition of 5 ml of lysis buffer, cells were mechanically scraped and homogenized in an ice-cold Dounce homogenizer (20 strokes by hand). The suspension was centrifuged at 43,000 × *g* for 10 min. The pellet was resuspended in the minimum volume of ice-cold 50 mM Tris/10 mM GCl_2/1 mM EDTA (pH 8.26 at 5°) buffer required for the binding assay and homogenized in a Dounce homogenizer. Typically, six to eight 175-cm^2 flasks were used for a 48-tube assay. ADA was added to a final concentration of 3 units/ml, and the suspension was incubated at 37 ° for 15 min; the membrane suspension was subsequently kept on ice until use. When large batches (~100 flasks) were processed homogenization was performed with a Polytron (Brinkman, Luzern, Switzerland), and further work-up was as described above. The preparation was stored at −70 ° and retained its [^{125}I] APNEA binding properties for at least 1 month.

Radioligand binding assay

Binding of [^{125}I]APNEA to CHO cells stably transfected with the rat A_3 receptor clone was performed essentially as described (6). Assays were performed in 50/10/1 buffer in glass tubes and contained 100 μl of the membrane suspension, 50 μl of [^{125}I] APNEA (final concentration 0.5 nM), and 50 μl of inhibitor. Inhibitors were routinely dissolved in Me_2SO and were then diluted with buffer; final Me_2SO concentrations never exceeded 1%. This concentration did not influence [^{128}I]APNEA binding. Incubations were carried out in duplicate for 1 hr at 37 ° and were terminated by rapid filtration over Whatman GF/B filters, using a Brandell cell harvester (Brandell, Gaithersburg, MD). Tubes were washed three times with 3 ml of buffer. Radioactivity was determined in a Beckman γ 5500B γ-counter. Nonspecific binding was determined in the presence of 40 μM *R*-PIA. K_i values were calculated according to Cheng and Prusoff (11), assuming a K_d for [^{125}I]APNEA of 17 nM (3).

The level of nonspecific binding with [^{125}I]APNEA in transfected CHO cells was 20–30%. There was some variability in the Hill coefficients (range from 0.8 to 1.2). Untransfected CHO cells displayed a low level of binding displacable by 100 μM *R*-PIA (at 5 nM [^{125}I]APNEA, only 5–10% of the level of specific A_3 binding in transfected cells), but this binding did not have pharmacological characteristics of adenosine receptors.

Binding of [^{3}H]PIA to A_1 receptors from rat brain membranes and of [^{3}H]CGS 21680 to A_{2a} receptors from rat striatal membranes was performed as described previously (9).

Adenylate cyclase assay

Adenylate cyclase was assayed in membranes from CHO cells stably expressing the rat A_3 receptor, prepared as above, using a modification of previously reported methods (18). Maximal inhibition of adenylate cyclase activity corresponded to ~40% of total activity under conditions of stimulation (typically by 6–8-fold) in the presence of 1 μM forskolin.

Membranes were resuspended in 75 mM Tris, 200 mM NaCl, 1.25 mM MgCl2, pH 8.12, at 4°C (TNM buffer) to give a final concentration of 0.1 mg/ml, and 2 units/ml adenosine deaminase was added. For the cyclase assay, the TMN buffer was supplemented with 140 μM dATP, 5 μM GTP, 30 units/ml creatine kinase, 5 mM creatine phosphate, 2.2 mM dithiothreitol, 100 μM papaverine, and 1.5 μCi of [α-^{32}P] ATP. Then 40 μl of the membrane suspension, 40 μl of the supplemented buffer, and 20 μl of a solution of forskolin

and the test compound (initially dissolved in Me_2SO then diluted in TMN buffer) were combined and incubated at 30 ° for 15 min, followed by termination by addition of a stop solution containing 20,000 cpm/ml [^{3}H]cyclic AMP. The final concentration of Me_2SO did not exceed 1%, which had no effect on adenylate cyclase. Labeled cyclic AMP was isolated by chromatography on Dowex 50 and alumina columns, and ^{32}P was measured using scintillation counting.

Molecular modeling

Structures were built using Quanta (version 3.3; Polygen, Waltham, MA), and molecular mechanics calculations were performed with CHARMm (version 21.2; Harvard College, Boston, MA), running on a Silicon Graphics Indigo XZ 4000 workstation. An A_3 receptor model was built with the model of the A_1 receptor we recently proposed as a starting point (12). The latter model is based on the well defined structure of the seven-transmembrane domain protein bacteriorhodopsin and assumes that the spatial orientation of the α-helical domains of G protein-coupled receptors is similar to that of bacteriorhodopsin. An initial structure for the A_3 receptor was generated by copying the backbone coordinates (and side chain coordinates where applicable) of the relevant residues in the A_1 model to their A_3 counterparts. Initial bad contacts within the individual helices were relieved by energy minimization using 200 steps of steepest descents, followed by 200 steps of an adopted basis Newton Raphson. Subsequently, the model was minimized using 500 steps of steepest descents, followed by an adopted basis Newton Raphson minimization until the rms energy gradient was less than 0.01 k_{cal}/mol Å, while keeping the backbone positions fixed. As a last step, the model was energy-minimized under the same conditions with backbone constraints of 5 k_{cal}/mol. Adenosine and other ligands were docked into the presumed binding site starting with the orientation that CPA assumes in the A_1 model (12), followed by a two-step energy minimization as described above. Calculations were performed using an extended atom approach and without explicit water, however, a distance-dependent dielectric constant was used to account for the screening effect of solvent.

Results and Discussion

SAR for adenosine derivatives

Binding data for a variety of adenosine derivatives, as well as a number of nucleosides having bases other than adenine are given in Table 1. Representative binding curves for three purine-substituted adenosine derivatives are shown in Fig. 1. The affinity of adenosine itself cannot be accurately determined in this binding assay, due to the presence of adenosine deaminase, which is required to degrade endogenously generated adenosine. Hence, it is not possible to directly compare the affinities of adenosine with the derivatives tested here. The affinity of adenosine has previously been estimated at 30 μM (3), but this value should be taken as only a rough approximation.

As is the case for A_1 receptors, the most potent compounds at the A_3 receptor are N^6-substituted and/or 5′-*N*-ethylcarboxamide-substituted adenosine derivatives. There are, however, profound differences between the N^6 topology of A_1 and A_3 receptors. In general, the affinities of N^6-substituted adenosines are much higher at A_1 than at A_3 receptors, with a few notable exceptions. It appears that the selectivity ratio is proportional to A_1 affinity; the higher the affinity at A_1, the higher the selectivity for A_1 versus A_3. This indicates that at the A_1 receptor, N^6 substituents can interact with a receptor region that is not present in the A_3 receptor. The stereoselectivity characteristic of the N^6 region of A_1 and A_2 receptors is maintained at A_3, albeit that *R*-PIA is only 6-fold more potent than *S*-PIA.

In a series of N^6-aryl(alkyl)-substituted compounds, N^6-benzyladenosine is more potent (K_i, 120 nM) than N^6-phenyladenosine (K_i, 802 nM) or N^6-phenethyladenosine (K_i, 240 nM).

This is surprising given the poor affinity of the former compound at A_1 (K_i, 120 nM) and at A_{2a} (K_i, 285 nM) receptors, whereas the phenyl and phenethyl derivatives have affinities in the lower nanomolar range at A_1 receptors (Table 1). Thus, N^6-benzyladenosine is essentially nonselective.

Another significant difference with A_1 and A_{2a} receptors is that introduction of a *p*-sulfo group in N^6-phenyladenosine slightly enhances affinity (N^6-(*p*-sulfophenyl)adenosine, K_i, 526 nM), in sharp contrast to A_1 and A_{2a} receptors, where a sulfo group drastically reduces affinity (Table 1). Two other N^6-sulfo derivatives, N^6-3-(4-sulfophenyl)propyladenosine and N^6-4-(4-sulfophenyl)butyladenosine have affinities in the same range (Table 1), but the 2-sulfoethyl derivative, which has a shorter N^6 substituent, is considerably less potent (K_i, 32.4 μM). Because the polar sulfo group is apparently better tolerated at A_3 than at A_1 and A_{2a} receptors, sulfo substitution shifts affinity in the direction of A_3 selectivity.

The A_1-selective N^6-cycloalkyl derivatives, CHA and CPA, are also among the more potent compounds at A_3 (K_i, 167 and 240 nM, respectively), as is the N^6-functionalized congener N^6-[4-[[[4-[[[(2-aminoethyl)amino]carbonyl]methyl]anilino]carbonyl]methyl]phenyl]adenosine (K_i, 281 nM). The A_2-selective N^6-substituted compound, N^6-[2-(3,5-dimethoxyphenyl)-2-(2-methylphenyl)ethyl]adenosine, has moderate potency at A_3 (K_i, 3.57 μM).

The affinity of N^6-dimethyladenosine is quite low (K_i, 32.5 μM), similar to the poor affinity of this compound at A_1 and A_{2a} receptors. The affinity of N^6-benzyl-N^6-methyladenosine and N^6-dimethylNECA is also considerably lower than the parent compounds N^6-benzyladenosine and NECA but not as drastically reduced as at A_1 and A_2 receptors. Thus, although disubstitution at N^6 reduces affinity, it enhances selectivity for A_3 versus A_1 and A_{2a} receptors (*e.g.*, N^6-dimethylNECA is 4-fold selective versus A_1 and 6-fold versus A_{2a}).

Similar to other adenosine receptor subtypes, NECA (5′-*N*-ethylcarboxamide adenosine) is relatively potent (K_i, 113 nM). However, unlike A_1 and A_{2a} receptors (10), the effects of N^6 and C5′ substitutions appear to reinforce each other. Thus, the 5′-*N*-ethylcarboxamide of CHA is considerably more potent than either CHA (K_i, 167 nM, 10-fold) or NECA (K_i, 113 nM, 7-fold), and, with a K_i of 16 nM, it is a highly potent compound at A_3 receptors. Likewise, N^6-dimethylNECA is 14-fold more potent than N^6-dimethyladenosine. These findings prompted us to synthesize the NECA analogue of N^6-benzyladenosine. Because N^6-benzyladenosine is more or less equipotent at all three subtypes, and the 5′-*N*-ethyl substituent apparently boosts affinity at A_3 receptors more than at A_1 and A_{2a}, it was expected that N^6-benzylNECA would be a potent and somewhat A_3-selective agonist. Indeed, N^6-benzylNECA has the highest A_3 affinity of all compounds tested in this study, with a K_i value of 6.8 nM, 18-fold more potent than the parent compound N^6-benzyladenosine. This is also the most A_3-selective compound found in the present study (13-fold versus A_1 and 14-fold versus A_{2a}). This compound may prove useful in the pharmacological characterization of A_3 receptors, *e.g.*, as a radioligand and as a lead for the further development of more selective A_3 agonists.

Certain C2 modifications may result in A_{2a}-selective agonists (1). At A_3 receptors, 2-chloroadenosine and 2-phenylaminoadenosine are of intermediate potency (K_i, 1.9 and 4.4 μM, respectively). An N^6-substituted derivative (2-chloro-N^6-CPA, K_i, 237 nM) and one bearing a 5′-*N*-ethylcarboxamide group (CGS 21680, K_i, 584 nM) are more potent C2-substituted derivatives. Thus, 2 substitution is tolerated to a degree at the A_3 receptor.

With regard to modifications of the ribose moiety, both the L-enantiomer and the α-anomer of adenosine are virtually inactive ($IC_{50} \gg 100$ μM), similar to other adenosine receptors (13). Psicofuranosyladenine, which contains an extra CH_2OH group at Cl′, is also very

weak. 2′-Deoxy-, 2′-*O*-methyl, and 3′-deoxyadenosine all have low affinity (IC_{50} > 100 μM), and inversion of the stereochemistry of the 2′-OH group (adenine-β-D-arabinofuranoside) similarly results in a low affinity compound. Thus, the presence of the 2′-OH in the S-configuration and the 3′-OH appears to be essential for high affinity. This has also been shown for other adenosine receptor subtypes (reviewed in Ref. 1). The 5′ position is more amenable to modifications than the 2′ or the 3′ position. The 5′-deoxy derivative of adenosine is moderately potent (K_i, 2.83 μM), and, as stated, the 5′-*N*-ethylcarboxamide derivative (NECA) is one of the more potent compounds tested (K_i, 113 nM). Some 5′-deoxyadenosine derivatives, including those with methylthio-, isobutylthio-, and methionine substituents have affinities in the lower micromolar range, whereas 5′-deoxy-5′-aminoadenosine and AMP (bearing a 5′-phosphate group) are virtually inactive IC_{50} > 100 μM. This parallels the affinities of these compounds at A_1 and A_{2a} receptors (Table 1). In all, ribose SAR for the A_3 receptor is comparable with A_1 and A_{2a} receptors, suggesting that the ribose domain may be quite similar in all three receptor subtypes.

Some adenosine derivatives not commonly used in adenosine receptor studies were tested. 6-Thiopurine riboside and 8-bromoadenosine both have low affinity (IC_{50} > 100 μM) at A_3, similar to A_1 and A_{2a} receptors. A bulky 8 substituent forces the ribose moiety in a predominantly *syn* conformation, which is a likely explanation for the inactivity of 8-bromoadenosine. The same has been shown for A_1 receptors (7). 7-Deazaadenosine has a $IC_{50} \gg 100$ μM, which indicates the importance of N^7. 3-Deazaadenosine is slightly more potent, with a K_i of 62 μM. l-Deazaadenosine was not available for testing, but 1-deaza-2-chloro-CPA, (K_i, 770 nM) is only 3-fold less potent than 2-chloro-CPA (K_i, 237 nM). This suggests that the presence of N^1 is not crucial, and it is consistent with the profile at other adenosine receptor subtypes, where N^1-deazaadenosine > N^3-deazaadenosine > N^7-deazaadenosine (reviewed in Ref. 1). The N^1-oxides of adenosine, NECA, and N^6-benzyladenosine are moderately potent compounds (K_i, 3.09, 0.47, and 7.25 μM, respectively) but less potent than at A_1 and A_{2a} receptors (Table 1).

Of the unsubstituted nonadenine nucleosides tested, only inosine (K_i, 45 μM) and guanosine (K_i, 99 μM) show some affinity for the A_3 receptor. The 5′-*N*-ethylcarboxamide derivative of inosine (NECI) is more potent (K_i, 5 μM), which is consistent with the affinity-enhancing effect of the 5′-carboxamido substituent of NECA. NECI is also selective for A_3 receptors, having an IC_{50} larger than 100 μM at A_1 and A_{2a} receptors. An adenosine transport inhibitor, (4-nitrobenzyl)-6-thioguanosine (K_i, 41 μM), is slightly more potent than the parent compound, guanosine.

SAR for nonadenosine derivatives

According to Zhou *et al.* (3), xanthines do not appear to displace [^{125}I]APNEA binding to A_3 receptors. We first tested a variety of nonxanthines known to act as antagonists at A_1 and/or A_{2a} receptors, including CGS 15943, CP 66713, 1*H*-imidazo[4,5-*c*]quinolinamine, 9-ethylcyclopentyladenine, and amiloride (Table 1). None of these appeared to be particularly potent, with K_i values in the range of 100 μM or larger. The adenosine deaminase inhibitor, *erythro*-9-(2-hydroxy-3-nonyl)adenine, was somewhat more potent with an IC_{50} slightly better than 100 μM (57.5% displacement at 100 μM), *erythro*-9-(2-Hydroxy-3-nonyl)adenine was of moderate affinity at A_1 receptors.

We therefore turned to a more detailed study of xanthine SAR (Table 1) than in the original paper (3). Xanthine was found to be a very weak displacer of [^{125}I]APNEA binding (14% at 100 μM). Substitutions at the 1 and the 3 positions enhance affinity. Compared with theophylline (1,3-dimethylxanthine, 23.1% at 100 μM), 1,3-dibutylxanthine is more potent (K_i, 143 μM). 1,3-Dihexylxanthine (9.2% at 10 μM) and 1,3-dibenzylxanthine (20.3% at 10 μM) also seem more potent than theophylline, but their limited solubility precludes direct

comparison. This profile is similar, but not identical, to other adenosine receptor subtypes, where propyl and butyl are optimal, and benzyl is slightly less potent (1). Still, even the most potent of these 1,3-substituted xanthines is quite weak at rat A_3 receptors.

Due to the limited solubility of even the most potent xanthine, it was not feasible to compare precisely the degree of maximal displacement of the xanthines and the adenosine derivatives. Unfortunately, the more water-soluble xanthines, such as XAC (positively charged at physiological pH) and 8-(*p*-sulfophenyl)-1,3-dipropylxanthine (negatively charged at physiological pH) did not bind appreciably to rat A_3 receptors.

Unlike A_1 and A_{2a} receptors, 8 substituents do not appear to contribute much to affinity and none of the 8-substituted xanthine derivatives tested is particularly potent (Table 1). This is surprising, because at A_1 and A_{2a} receptors, affinities of N^6-substituted adenosines and xanthines similarly substituted at the 8 position closely parallel each other, suggesting that N^6 and C8 substituents interact with the same receptor domain (1, 14). Clearly, this is a subject for further investigation. Substitutions at the 7 position appear to be tolerated, in contrast to A_1 receptors, where 7 substituents tend to diminish affinity (7); *e.g.*, both caffeine and 7-benzyltheophylline are slightly more potent at A_3 receptors than the 7-unsubstituted parent compound, theophylline. The A_{2a}-selective antagonist 8-(3-chlorostyryl)caffeine (47) did not inhibit binding at rat A_3 receptors.

Molecular modeling and prediction of affinity of xanthine-7-ribosides

Like other G protein-coupled receptors, the amino acid sequence of A_3 receptors contains seven hydrophobic stretches of approximately 25 residues that are believed to traverse the cell membrane as α-helices (3). No detailed three-dimensional structures (X-ray or NMR) for any of the G protein-coupled receptors are known, but it is now well accepted that the structure of bacteriorhodopsin, which has been solved by cryo-electron microscopy (15), is a suitable starting point for the modeling of G protein-coupled receptors (16). We have recently described a model for the A_1 adenosine receptor (12), and, here, we present a similar model for the A_3 receptor. Details of the building of the model are given under Materials and Methods.

A close-up of the proposed binding site of the A_3 receptor with N^6-benzyladenosine as the ligand is shown in Fig. 2. This model is based on pharmacological observations and analogies with the A_1 receptor and is consistent with the SAR described above. N^6-Benzyladenosine was chosen as a typical agonist for the A_3 receptor, because it is relatively potent (Table 1). In the A_1 model (12), CPA was chosen as a typical high affinity A_1-selective agent for the purpose of docking to the binding site. There, CPA is coordinated by two histidine residues in helices VI and VII, whose involvement is in full agreement with both chemical modification studies (17) and site-directed mutagenesis (18). It should be mentioned here that another quite different A_1 receptor model has been developed in which no specific interaction with histidine residues was proposed (48).

There are a number of similarities as well as some substantial differences between our models for the A_1 and A_3 receptors. As in the A_1 model, the agonist ligand is present in the *anti* conformation (χ, the torsion angle of the glycosidic bond is 76°), consistent with earlier modeling and NMR studies (19). The model proposes several points of interaction between the receptor and the ribose moiety. Hydrogen bonds could be formed between the 2′- and 3′-OH groups and His^{274} in helix VII and between the 5′-OH group and Ser^{277} in helix VII. There are equivalent interactions with His^{278} and Ser^{281} in the A_1 receptor model. Thus, the ribose binding domain seems to be quite similar for A_3 and A_1 receptors, in good agreement with the agonist SAR described here; the same appears to be true for A_{2a} receptors (45). In the present model, the side chain of Phe^{184} (helix V) is located near the glycosidic bond of

receptor-bound N^6-benzyladenosine. The same Phe residue and Thr[96] (helix III) appear to be in proximity to the C5′ region.

A major structural difference is that the A_3 receptor does not contain the histidine residue in helix VI that is common to all A_1 and A_2 receptors cloned so far (20) and that has been shown to have an effect on both agonist and antagonist binding to A_1 receptors (18). In particular, the His of helix VI has been shown to be important for antagonist affinity, a finding that suggests a linkage between the absence of this His residue and the lack of high affinity binding of antagonists such as XAC at rat A_3 receptors. In the model of agonists binding to A_1 receptors (12), this residue forms a hydrogen bond with N^6-H. In the A_3 receptor, a serine residue (Ser[249]) is found in the analogous position, and it could be argued that serine could serve a similar function as a hydrogen bond acceptor. However, due to a different orientation of the purine moiety in the A_3 binding site, this serine seems to be too far from N^6-H (~7 Å) to be able to form this bond. The reason for the different orientation is as follows. The majority of the amino acid residues that are different between A_1 and A_3 receptors occur in the immediate vicinity (within 5 Å) of the agonist ligand, and many of the A_3 residues are considerably more bulky (*e.g.*, Phe[95]) than their A_1 counterparts. This results in a ligand binding environment (for both the purine and ribose domains) that is much more constricted than is the case for the A_1 receptor (12). In Fig. 3 the binding orientations of CPA to the A_1 receptor and of N^6-benzyladenosine to the A_3 receptor are shown to illustrate these differences. They provide a tentative explanation for the apparent low affinity of xanthines and nonxanthine A_1/A_2 antagonists. In addition, the ribose moiety that likely serves to anchor the native ligand adenosine to the receptor is absent in these compounds.

As in the A_1 model, a hydrophobic pocket directed toward the extracellular space, capable of accommodating large N^6 substituents, is present. Fig. 2 shows the binding environment of the benzyl substituent of N^6-benzyladenosine. Indeed, a number of N^6-substituted adenosine derivatives, including the long chain functionalized congener N^6-[4-[[[4-[[[(2-aminoethyl)amino]carbonyl]methyl]anilino]carbonyl]methyl]-phenyl]adenosine, have considerable affinity for the A_3 receptor (Table 1). Amino acid residues in proximity to the N^6-benzyl ring according this model are the side chains of Phe[181] (hydrophobic) and Asp[177] (anionic) and the backbone atoms of Tyr[178] (all in helix V). Due to the rather constricted agonist binding domain, the N^6 region is much closer to the membrane surface than in the A_1 model. It might be hypothesized that the paucity of hydrophobic residues for an N^6 substituent to interact with, because of the proximity of the N^6 region to the membrane surface, accounts for the rather moderate affinity of N^6-substituted adenosines, in comparison with the much higher affinities of a number of similar agonists at A_1 and A_{2a} receptors. This would also agree well with a polar sulfo substituent being tolerated close to the N^6 region of A_3 but not A_1 or A_{2a} receptors. A second (hydrophobic) pocket is present adjacent to C2, which can accommodate fairly large C2 substituents. Again, this agrees well with the considerable potency of some C2-substituted agonists, *e.g.*, CGS 21680 (Table 1). The backbone of Tyr[256] (helix VI) is situated near the purine C2 position of N^6-benzyladenosine.

It should be noted here that due to the relative scarcity of pharmacological and structural data for this novel receptor, of necessity, there are uncertainties in this model. The question about the involvement of Ser[249] in binding of the purine moiety and whether the different agonist orientations in the A_1 and A_3 models will hold up should be addressed experimentally. Chemical modification studies, site-directed mutagenesis, and more SAR work will be needed to further define essential characteristics of the ligand-receptor interaction, which, in turn, may lead to a more refined model. At this stage, the A_3 model

should mainly be seen as a starting point to generate ideas for experiments, and its usefulness is illustrated by the following.

The notion from the modeling studies that the primary point of interaction between receptor and ligand appears to be the ribose moiety of agonists, combined with the observation that 7 substitution apparently is tolerated, prompted us to test some xanthine-7 ribosides that were previously synthesized (7). It was reasoned that the ribose hydroxyl groups might serve to anchor the xanthine nucleus to the receptor. Indeed, of the compounds tested, 1,3-dibutylxanthine-7 riboside (DBXR) was quite potent (K_i, 6μM), almost 25-fold more potent than the parent 1,3-dibutylxanthine, which was one of the most potent xanthines tested (Table 1). Affinity at A_1 and A_{2a} receptors is 4.19 and 19.5 μM, respectively, so this compound has only very moderate selectivity.

Fig. 4 illustrates a proposed model for DBXR binding to the A_3 receptor. According to this model, the 1,3-dialkyl substituents of DBXR are located in hydrophobic regions near the exofacial surface of the A_3 receptor. Specifically, the N^1 -butyl chain is located near the side chain of Tyr^{256} of helix VI, and the N^3-butyl chain is located near the side chain of Phe^{181} of helix VI.

Effects on adenylate cyclase

The effects of key compounds on the inhibition of adenylate cyclase in CHO cells stably expressing the rat A_3 receptor was measured (Fig. 5). Indeed, adenosine derivatives N^6-cyclohexylNECA and N^6-benzylNECA proved to be agonists at A_3 receptors, with full efficacy, as observed with *R*-PIA and NECA (data not shown). The maximal inhibition of adenylate cyclase elicited by N^6-cyclohexylNECA was 45.7 ± 2.1%. The IC_{50} determined for this compound was 1.30 ± 0.31 μM. N^6-BenzylNECA was nearly as potent (IC_{50} 1.61 μM) with a maximal inhibition of 47.6 ± 6.3%.

At A_1 receptors, xanthine-7 ribosides have been shown to act as antagonists or partial agonists (7, 21). At rat A_3 receptors, 1,3-dibutylxanthine-7 riboside did inhibit adenylate cyclase, but the dose-response curve was more shallow than for the adenosine derivatives (only 20.9 ± 4.0% inhibition at 100 μM); thus, it appears to be a partial agonist. The inosine derivative NECI was so weak in inhibiting adenylate cyclase that a full-dose response was not able to be measured; at a concentration of 10^{-4} M, it inhibited adenylate cyclase by 9.4 ± 3.8% (n = 7). Although the majority of the compounds were not assayed in this functional assay, the rank order of potency paralleled the order of potency in displacing the specific binding of radioligand at A_3 receptors.

1,3-Dibutylxanthine at 100 μM neither antagonized the action of an adenosine agonist (N^6-cyclohexylNECA) acting at A_3 receptors nor itself inhibited adenylate cyclase in the transfected CHO cells. Theophylline was also unable to antagonize the inhibition of adenylate cyclase elicited by N^6-benzylNECA. N^6-BenzylNECA alone had an IC_{50} value of 1.35 ± 0.65 μM, with maximal inhibition of 28.8 ± 0.9% (100 μM). In the presence of 1 mM theophylline, the IC_{50} value was 0.91 ± 0.1 μM, with a maximal inhibition of 34.2 ± 1.5%. Theophylline had no effect on the basal level of adenylate cyclase or on how much forskolin was able to stimulate.

Conclusions

N^6-BenzylNECA was identified as the first highly potent and moderately A_3-selective agonist. Combined with the other SAR differences found between A_3 and A_1/A_2 affinity, such as polar substituents being tolerated in the N^6 region, it should provide a good lead toward the development of even more potent and selective A_3 agonists.

Mutation experiments have shown that the His residue in the sixth transmembrane helix of both A_1 and A_2 receptors is involved in the high affinity binding of antagonists such as XAC (18). The complete inactivity of xanthines at rat A_3 receptors, which lack that His, is consistent with this model. This A_3 receptor molecular model has also been in part validated with the moderate affinity of 1,3-dibutylxanthine-7 riboside, which appears to act as a partial agonist. This study did not identify any A_3 antagonists among a wide range of the known A_1/A_2 receptor antagonists.

The predictions of the computer-generated model for the binding site must be tested through further efforts in ligand synthesis and modification of the receptor structure through site-directed mutagenesis of A_3 receptors. More elaborate SAR studies to further define optimal substituents for interaction with the N^6 and C5′ regions of the A_3 adenosine receptor are currently underway.

Acknowledgments

We thank Dr. Arthur Jacobson and the Scientific Resources Computer Center at the National Institutes of Health for use of computer facilities and Drs. John Daly and Bilha Fischer for useful suggestions.

ABBREVIATIONS

APNEA	N^6-2-(4-aminophenyl)ethyladenosine
CGS 15943	9-chloro-2-(2-furyl)[1,2,4]triazolo[1,5-*c*]quinazolin-5-amine
CGS 21680	2-[4-(2-carboxyethyl)phenyl]ethylamino-5′-*N*-ethlcarboxamidoadenosine
CHA	N^6-cyclohexyladenosine
CPA	N^6-cyclopentyladenosine
DBXR	1,3-dibutylxanthine-7 riboside
NECA	5′-*N*-ethylcarboxamidoadenosine
NECI	5′-*N*-ethylcarboxamidoinosine
***R/S*-PIA**	N^6-[(*R*/*S*)-1-methyl-2-phenylethyl]adenosine
SAR	structure-activity relationships
XAC	8-[-4-[[[[(2-aminoethyl)amino]carbonyl]methyl]oxy]phenyl]-1,3-dipropylxanthine
Me_2SO	dimethylsulfoxide
CHO	Chinese hamster ovary

References

1. van Galen PJM, Stiles GL, Michaels G, Jacobson KA. Adenosine A_1 and A_2 receptors: structure-function relationships. Med Res Rev. 1992; 12:423–471. [PubMed: 1513184]
2. Jacobson KA, van Galen PJM, Williams M. Perspective. Adenosine receptors: pharmacology, structure-activity relationships and therapeutic potential. J Med Chem. 1992; 35:407–422. [PubMed: 1738138]
3. Zhou QY, Li CY, Olah ME, Johnson RA, Stiles GL, Civelli O. Molecular cloning and characterization of an adenosine receptor: the A_3 adenosine receptor. Proc Natl Acad Sci U S A. 1992; 89:7432–7436. [PubMed: 1323836]

4. Meyerhof W, Müller-Brechlin R, Richter D. Molecular cloning of a novel putative G protein-coupled receptor expressed during rat spermiogenesis. FEBS Lett. 1991; 284:155–160. [PubMed: 1647979]
5. Ramkumar V, Stiles GL, Beaven MA, Ali H. The A_3 adenosine receptor is the unique adenosine receptor which facilitates release of allergic mediators in mast cells. J Biol Chem. 1993; 268:16887–16890. [PubMed: 8349579]
6. Stiles GL, Daly DT, Olsson RA. The A_1 adenosine receptor. Identification of the binding subunit by photoaffinity cross-linking. J Biol Chem. 1985; 260:10806–10811. [PubMed: 2993290]
7. van Galen PJM, Ijzerman AP, Soudijn W. Xanthine-7 ribosides as adenosine receptor antagonists. Nucleos Nucleot. 1990; 9:275–291.
8. van Galen PJM, Nissen P, van Wijngaarden I, Ijzerman AP, Soudijn W. ^{1}H-imidazo(4,5-*c*]qninolin-4-amines: novel nonxanthine adenosine antagonists. J Med Chem. 1991; 34:1202–1206. [PubMed: 2002461]
9. Jacobson KA, Nikodijevic O, Ji XD, Berkich DA, Eveleth D, Dean RL, Hiramatsu K, Kassell NF, van Galen PJM, Lee KS, Bartus RT, Daly JW, Lanoue KF, Maillard M. Synthesis and biological activity of N^6-(*p*-sulfophenyl)alkyl and N^6-sulfoalkyl derivatives of adenosine. Water-soluble and peripherally selective adenosine agonists. J Med Chem. 1992; 35:4143–4149. [PubMed: 1433217]
10. Olsson RA, Kusachi S, Thompson RD, Ukena D, Padgett W, Daly JW. N^6-substituted *N*-alkyladenosine-5′-uronamides: bifunctional ligands having recognition groups for A_1 and A_2 adenosine receptors. J Med Chem. 1986; 29:1683–1689. [PubMed: 3018244]
11. Cheng YC, Prusoff WH. Relationship between the inhibition constant (K_i) and the concentration of inhibitor which causes 50 percent inhibition (IC_{50}) of an enzyme reaction. Biochem Pharmacol. 1973; 22:3099–3108. [PubMed: 4202581]
12. Ijzerman AP, van Galen PJM, Jacobson KA. Molecular modeling of adenosine receptors. I. The ligand binding site on the A_1 receptor. Drug Design Dev. 1992; 9:49–68.
13. Brims RF. Adenosine receptor activation in human fibroblasts: nucleoside agonists and antagonists. Can J Physiol Pharmacol. 1980; 58:673–691. [PubMed: 6253037]
14. van der Wenden EM, Ijzerman AP, Soudijn W. A steric and electrostatic comparison of 3 models for the agonist/antagonist binding site on the adenosine A_1 receptor. J Med Chem. 1992; 35:629–635. [PubMed: 1542091]
15. Henderson R, Baldwin JM, Ceska TA, Zemlin F, Beckman E, Downing KH. Model for the structure of bacteriorhodopsin based on high resolution electron cryo-microscopy. J Mol Biol. 1990; 213:899–929. [PubMed: 2359127]
16. Hibert MF, Trumpp-Kallmeyer S, Hoflack J, Bruinvels A. This is not a G protein-coupled receptor. Trends Pharmacol Sci. 1993; 14:7–12. [PubMed: 8095116]
17. Klotz KN, Lohse MJ, Schwabe U. Chemical modification of A_1 adenosine receptors in rat brain membranes. Evidence for histidine in different domains of the ligand binding site. J Biol Chem. 1988; 263:17522–17526. [PubMed: 3182861]
18. Olah ME, Ren HZ, Ostrowski J, Jacobson KA, Stiles GL. Cloning, expression, and characterization of the unique bovine-A_1 adenosine receptor. Studies on the ligand binding site by site-directed mutagenesis. J Biol Chem. 1992; 267:10764–10770. [PubMed: 1587851]
19. van Galen PJM, Ijzerman AP, Soudijn W. Xanthine-7 ribosides as adenosine receptor antagonists. Further evidence for adenosine's anti mode of binding. Nucleos Nucleot. 1991; 10:1191–1193.
20. Linden J, Tucker AL, Robeva AS, Graber SG, Munshi R. Properties of recombinant adenosine receptors. Drug Dev Res. 1993; 28:232–236.
21. Borea PA, Varani K, Gardenghi A, Bertolasi V, van Galen PJM, Ijzerman AP. Theophylline-7 riboside: a partial agonist for adenosine A_1, receptors. Int J Purine Pyrimidine Res. 1992; 3:65.
22. Daly, JW.; Jacobson, KA. Molecular probes for adenosine receptors. In: Ribeiro, JA., editor. Adenosine Receptors in the Nervous System. Taylor & Francis; London: 1989. p. 41-52.
23. Bruns RF, Lu GH, Pugsley TA. Characterization of the A_2 adenosine receptor labeled by [^{3}H]NECA in rat striatal membranes. Mol Pharmacol. 1986; 29:331–346. [PubMed: 3010074]
24. Bridges AJ, Moos WH, Szotek DL, Trivedi BK, Bristol JA, Heffher TG, Bruns RF, Downs DA. N^6-(2,2-diphenylethyl)adenosine, a novel adenosine receptor agonist with antipsychotic-like activity. J Med Chem. 1987; 30:1709–1711. [PubMed: 2888894]

25. Trivedi, BK. Structure-activity relationships for adenosine agonists. In: Jacobson, KA.; Daly, JW.; Manganiello, V., editors. Purines in Cellular Signalling. Targets for New Drugs. Springer; New York: 1990. p. 136-145.
26. Cristalli G, Franchetti P, Grifantini M, Vittori S, Klotz KN, Lohse MJ. Adenosine receptor agonists: synthesis and biological evaluation of 1-deaza analogues of adenosine derivatives. J Med Chem. 1988; 31:1179–1183. [PubMed: 3373486]
27. Thompson RD, Secunda S, Daly JW, Olsson RA. Activity of N^6-2-chloroadenosines at A_1 adenosine and A_2 adenosine Receptors. J Med Chem. 1991; 34:3388–3390. [PubMed: 1766003]
28. Francis JE, Webb RL, Ghai GR, Hutchison AJ, Moskal MA, Dejesus R, Yokoyama R, Rovinski SL, Contardo N, Dotson R, Barclay B, Stone GA, Jarvis MF. Highly selective adenosine- A_2 receptor agonists in a series of *N*-alkylated 2-aminoadenosines. J Med Chem. 1991; 34:2570–2579. [PubMed: 1875349]
29. Daly JW, Padgett WL. Agonist activity of 2- and 5′-substituted adenosine analogs and their N^6-cycloalkyl derivatives at A_1-adenosine and A_2-adenosine receptors coupled to adenylate cyclase. Biochem Pharmacol. 1992; 43:1089–1093. [PubMed: 1554381]
30. Cristalli G, Grifantini M, Vittori S. Adenosine and 2-chloroadenosine deaza analogues as adenosine receptor antagonists. Nucleos Nucleot. 1985; 4:625–639.
31. Lohse MJ, Klotz KN, Diekmann E, Friedrich K, Schwabe U. 2′,3′-Dideoxy-N^6-cyclohexyladenosine: an adenosine derivative with antagonist properties at adenosine receptors. Eur J Pharmacol. 1988; 156:157–160. [PubMed: 3208837]
32. Sarges R, Howard HR, Browne RG, Lebel LA, Seymour PA, Koe BK. 4-Amino[l,2,4]triazolo[4,3-*a*]quinoxalines. A novel class of potent adenosine receptor antagonists and potential rapid-onset antidepressants. J Med Chem. 1990; 33:2240–2254. [PubMed: 2374150]
33. Francis JE, Cash WD, Psychoyos S, Ghai G, Wenk P, Friedmann RC, Atkins C, Warren V, Furness P, Hyun JL, Stone GA, Desai M, Williams M. Structure-activity profile of a series of novel triazoloquinazoline adenosine antagonists. J Med Chem. 1988; 31:1014–1020. [PubMed: 3361572]
34. Thompson RD, Secunda S, Daly JW, Olsson RA. N^6,9-Disubstituted adenines. Potent, selective antagonists at the A_1-adenosine receptor. J Med Chem. 1991; 34:2877–2882. [PubMed: 1895305]
35. Garritsen A, Ijzerman AP, Tulp MT, Cragoe EJ, Soudijn W. Receptor binding profile of amiloride provides no evidence for a link between receptor and the Na^+/H^+ exchanger but indicates a common structure on receptor proteins. J Recept Res. 1991; 11:891–907. [PubMed: 1661335]
36. Schwabe U, Ukena D, Lohse MJ. Xanthine derivatives as antagonists at A_1 and A_2 adenosine receptors. Naunyn Schmiedebergs Arch Pharmacol. 1985; 330:212–221. [PubMed: 2997628]
37. Shamim MT, Ukena D, Padgett WL, Daly JW. Effects of 8-phenyl and 8-cycloalkyl substituents on the activity of mono-, di-, and trisubstituted alkylxanthines with substitution at the 1, 3, and 7 positions. J Med Chem. 1989; 32:1231–1237. [PubMed: 2724296]
38. Daly JW, Butts-Lamb P, Padgett W. Subclasses of adenosine receptors in the central nervous system: interaction with caffeine and related methylxanthines. Cell Mol Neurobiol. 1983; 3:69–80. [PubMed: 6309393]
39. Daly JW, Padgett WL, Shamim MT. Analogues of caffeine and theophylline: effect of structural alterations on affinity at adenosine receptors. J Med Chem. 1986; 29:1305–1308. [PubMed: 3806581]
40. Schneller SW, Ibay AC, Christ WJ, Bruns RF. Linear and proximal benzo-separated alkylated xanthines as adenosine-receptor antagonists. J Med Chem. 1989; 32:2247–2254. [PubMed: 2795597]
41. Daly JW, Hide I, Bridson PK. Imidazodiazepinediones: a new class of adenosine receptor antagonists. J Med Chem. 1990; 33:2818–2821. [PubMed: 2213834]
42. Linden J. Structure and function of A_1 adenosine receptors. FASEB J. 1991; 5:2668–2676. [PubMed: 1916091]
43. Jacobson KA, Kirk KL, Padgett WL, Daly JW. Functionalized congeners of 1,3-dialkylxanthines: preparation of analogues with high affinity for adenosine receptors. J Med Chem. 1985; 28:1334–1340. [PubMed: 2993622]

44. Fozard JR, Carruthere AM. Adenosine A_3 receptors mediate hypotension in the angiotensin II-supported circulation of the pithed rat. Br J Pharmacol. 1993; 109:3–5. [PubMed: 8495245]

45. Ijzerman AP, van der Wenden EM, van Galen PJM, Jacobson KA. Molecular modeling of adenosine receptors. II. The ligand binding site on the A_2 receptor. Eur J Pharmacol. in press.

46. Jacobson KA, Shi D, Gallo-Rodriguez C, Manning M, Müller C, Daly JW, Neumeyer JL, Kiriasis L, Pfleiderer L. Effect of trifluoromethyl and other substituents on activity of xanthines at adenosine receptors. J Med Chem. 1993; 36:2639–2644. [PubMed: 8410976]

47. Jacobson KA, Gallo-Rodriguez C, Melman N, Fischer B, Maillard M, van Bergen A, van Galen PJM, Karton Y. Structure-activity relationships of 8-styrylxanthines as A_2-selective adenosine antagonists. J Med Chem. 1993; 36:1333–1342. [PubMed: 8496902]

48. Dudley MW, Peet NP, Demeter DA, Weintraub HJR, Ijzerman AP, Nordvall G, van Galen PJM, Jacobson KA. Adenosine A_1 receptor and ligand molecular modeling. Drug Dev Res. 1993; 28:237–243.

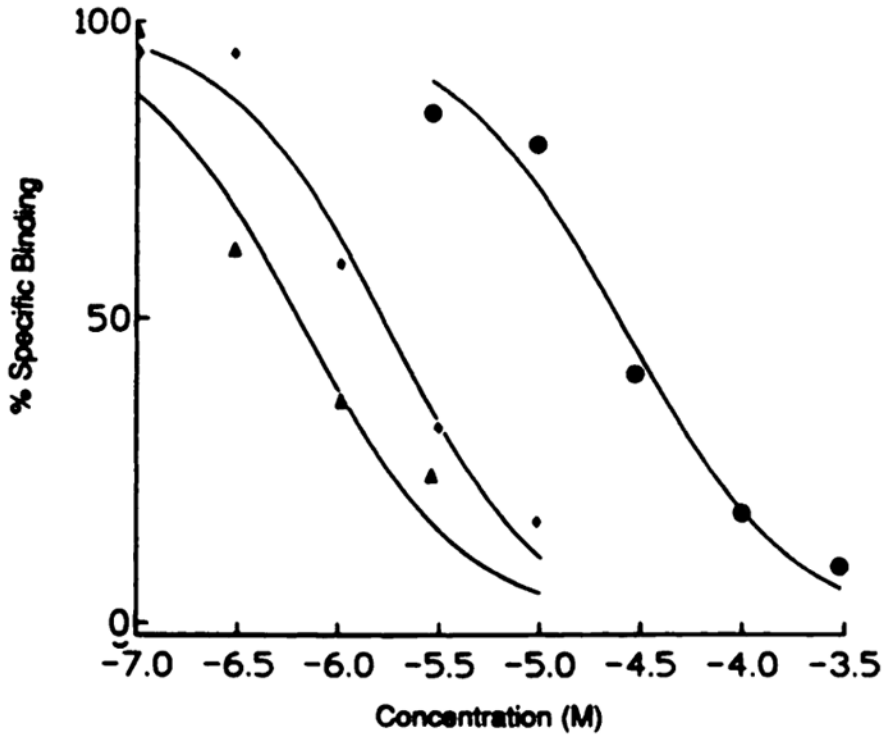

Fig. 1.

Displacement by three purine-modified adenosine analogues of specific binding of [^{125}I]APNEA (0.5 nM) from membranes from CHO cells transfected with rat A_3 receptors. The assay was carried out as described under Materials and Methods. Competitors were as follows (Hill coefficients in parentheses): ◆,2-chloroadenosine (1.10); △, 1-deaza-2-chloro-N^6-cyclotopentyladenosine (1.07); and ●, inosine (1.03). The *curves* are representative of single experiments in which each point is determined in triplicate.

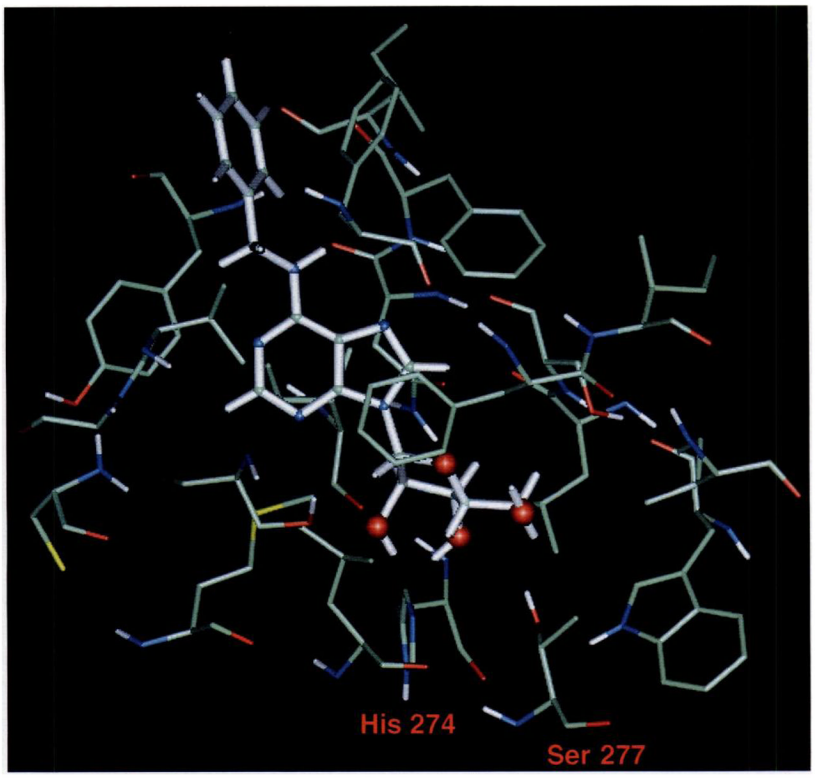

Fig. 2.

The proposed adenosine binding site of the A_3 receptor, with N^6-benzyladenosine as the ligand. The ligand is shown as a ball-and-stick representation (*thick bonds*) and the receptor is shown in liquorice bond style (*thinner bonds*). The 2′- and 3′-OH may form a hydrogen bond with His^{274}, and 5′-OH can form a hydrogen bond with Ser^{277}.

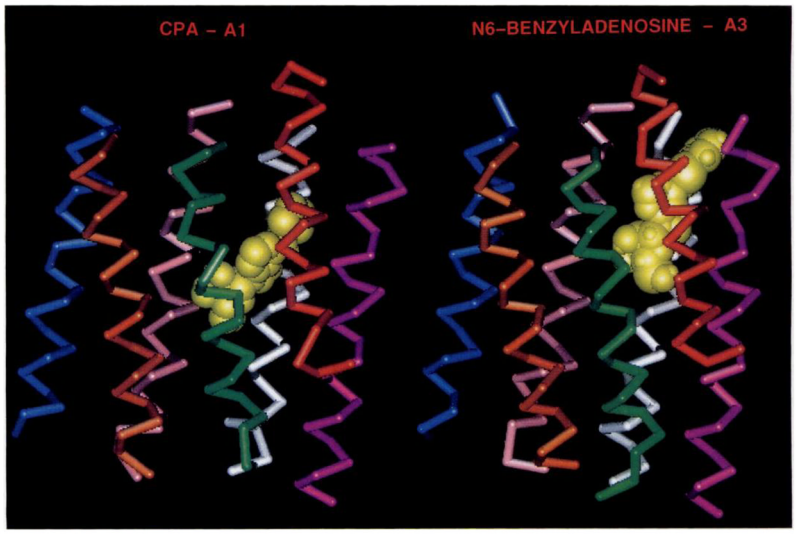

Fig. 3.

Comparison of CPA as bound in the A_1 model (*left*) and N^6-benzyladenosine in the A_3 model (*right*). Color coding is as follows: *yellow,* ligand; *blue,* H.I; *orange*, H.II; *green*, H.III; *red*, H.IV; *purple*, H.V; *white,* H.VI; *pink*, H.VII. The A_1 model is identical to that proposed in Ref. 12. See Results for a discussion of specific residues proposed to be in proximity to the bound N^6-benzyladenosine.

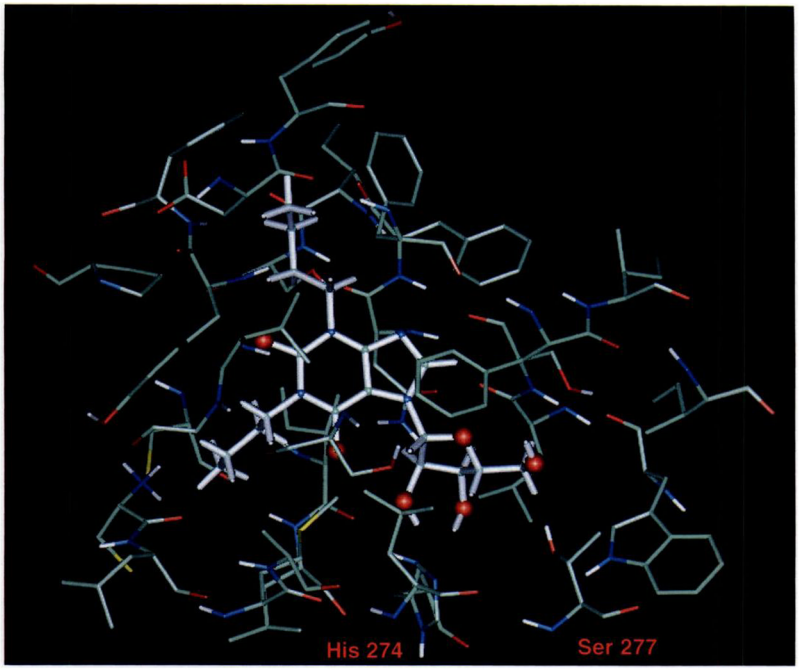

Fig. 4.

Proposed mode of binding of 1,3-dibutylxanthine-7-riboside to the A_3 receptor. Details are as for Fig. 1. The N^1-butyl chain is located near the side chain of Tyr^{256} of helix VI, and the N^3-butyl chain is located near the side chain of Phe^{181} of helix VI.

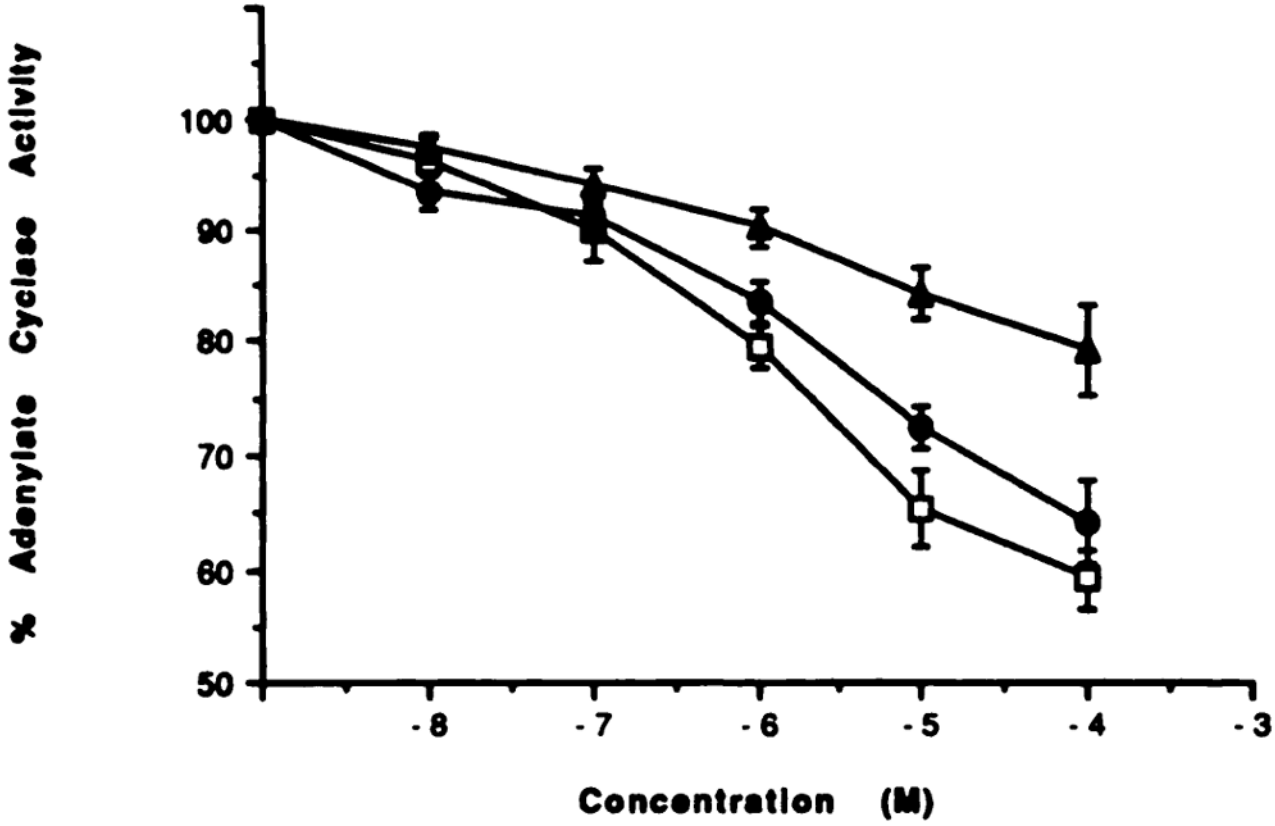

Fig. 5.

Inhibition of adenylate cyclase in membranes from CHO cells transfected with rat A_3 receptors. The assay was carried out as described under Materials and Methods. Each data point is shown as mean ± S.E. for four to seven determinations. Agents were as follows (number of separate experiments in parentheses): *triangles,* 1,3-dibutylxanthine-7-riboside (5); *circles,* N^6-benzylNECA (7); and *squares*, N^6-cyclohexyl-NECA (4). In these cell membranes, a K_D value for binding of [^{125}I]APNEA to A_3 receptors was 5.67 ± 0.73 nM with a B_{max} of 1.51 ± 0.40 pmol/mg protein.

TABLE 1

Affinities of selected compounds at A_1 A_{2a} and A_3 receptors, indicated as either K_i, (nM) or percent displacement at a concentration of 100 μM, unless otherwise indicated

Values expressed as means ± S.E. were all measured in this study (three to five experiments). K_i, values at A_1 and A_{2a} receptors provided without S.E. are taken from the literature as indicated.

Compound	A_1 affinity[a]	A_{2a} affinity[b]	A_3 affinity[c]	Reference
Purine and 5′-modified adenosines				
1. ADAC[d]	0.85 nM	210 nM	281 ± 51 nM	(22)
2. *R*-PIA	1.2 nM	124 nM	158 ± 52 nM	(23)
3. *S*-PIA	49.3 nM	1,820 nM	920 ± 311 nM	(23)
4. CPA	0.59 nM	462 nM	240 ± 36 nM	(23)
5. CHA	1.3 nM	514 nM	167 ± 26 nM	(23)
6. N^6-Phenyladenosine	4.62 nM	663 nM	802 ± 279 nM	(23)
7. N^6-Benzyladenosine	120 nM	285 nM	120 ± 20 nM	(23)
8. N^6-Phenethyladenosine	12.7 nM	161 nM	240 ± 58 nM	(24)
9. N^6-Dimethyladenosine	10,000 nM	28,900 ± 8,500 nM	32,500 ± 5,100 nM	(10)
10. DPMA	142 nM	4.4 nM	3,570 ± 1,700 nM	(25)
11. N^6-(2-Sulfoethyl)adenosine	41%	0%	32,400 ± 7,600 nM	(9)
12. N^6-(*p*-Sulfophenyl)adenosine	74 nM	8,900 nM	526 ± 142 nM	(9)
13. N^6-3-(*p*-Sulfophenyl)propyladenosine	610 nM	3,840 nM	844 ± 67 nM	(9)
14. N^6-4-(*p*-Sulfophenyl)butyladenosine	432 nM	11,300 nM	808 ± 116 nM	(9)
15. 1-Deaza-2-chloro-N^6-CPA	1.6 nM	13,200 nM	770 ± 234 nM	(26)
16. 2-Chloroadenosine	9.3 nM	63 nM	1,890 ± 900 nM	(23)
17. 2-Chloro-N^6-CPA	0.6 nM	950 nM	237 ± 71 nM	(27)
18. 2-(Phenylamino)adenosine	560 nM	119 nM	4,390 ± 1,170 nM	(23)
19. CGS 21680	2,600 nM	15 nM	584 ± 32 nM	(28)
20. NECA	6.3 nM	10.3 nM	113 ± 34 nM	(23)
21. N^6-CyclohexylNECA	0.43 nM	170 nM	16.0 ± 5.4 nM	(29)
22. N^6-BenzylNECA	87.3 ± 13.9 nM	95.3 ± 24.6 nM	6.8 ± 2.5 nM	
23. N^6-DimethylNECA	9,600 nM	13,500 ± 3,600 nM	2,260 ± 490 nM	(10)
24. N^6-Benzyl-N^6-methyladenosine	7,600 ± 1,900 nM	40,100 ± 6,200 nM	78.4 ± 4.6%	
25. 8-Bromoadenosine	41.5 ± 3.2%	22,700 ± 5,100 nM	31.3 ± 6.0%	
26. 3-Deazaadenosine	21,500 nM	59,800 ± 4,600 nM	61,700 ± 34,500 nM	(30)
27. 7-Deazaadenosine (tubercidine)	>100,000 nM	48.3 ± 0.4%	38.9 ± 17.7%	(30)
28. Adenosine-N^1-oxide	246 ± 31 nM	328 ± 60 nM	3,090 ± 1,910 nM	
29. NECA-N^1-oxide	154 ± 20 nM	101 ± 19 nM	468 ± 58 nM	
30. N^6-Benzyladenosine-N^1-oxide	864 ± 88 nM	8,530 ± 1,250 nM	7,250 ± 1,680 nM	
ribose-modified adenosines				
31. β-L-Adenosine	29,000 ± 4,700 nM	25.4 ± 1.1%	9.5 ± 4.2%	
32. α-D-Adenosine	350,000 nM	128,000 ± 25,000 nM	14.2 ± 6.5%	(31)
33. 2′-Deoxyadenosine	30.9 ± 8.0%	38.9 ± 2.9%	28.3 ± 2.3%	

Compound	A_1 affinity[a]	A_{2a} affinity[b]	A_3 affinity[c]	Reference
34. 2′-*O*-Methyladenosine	29.4 ± 7.5%	49.0 ± 5.0%	42.9 ± 9.4%	
35. 3′-Deoxyadenosine (cordycepin)	5.8 ± 2.8%	26.3 ± 3.4%	32.7 ± 2.0%	
36. 5′-Deoxyadenosine	269 ± 135 nM	596 ± 54 nM	2,830 ± 460 nM	
37. 5′-Deoxy-5′-aminoadenosine	42,700 ± 6,000 nM	38,500 ± 3,800 nM	20.6 ± 2.2%	
38. 5′-Deoxy-5′-methylthioadenosine	281 nM	1,100 nM	1,420 ± 530 nM	(23)
39. 5′-Deoxy-5′-isobutylthioadenosine	1,140 ± 130 nM	6,890 ± 1,750 nM	3,630 ± 360 nM	
40. *S*-Adenosylmethionine	675 ± 87 nM	2,780 ± 250 nM	2,470 ± 450 nM	
41. AMP	_*	57.5 ± 4.0%	17.2 ± 6.3%	
42. Adenine-β-D-arabinofuranoside	20.2 ± 8.4%	26.0 ± 8.4%	23.7 ± 3.8%	
43. β-D-Psicofuranosyladenine	36.1 ± 4.9%	51.5 ± 7.4%	21.1 ± 0.9%	
non-adenosine nucleosides				
44. Xanthosine	9.1 ± 2.4%	8.5 ± 2.5%	23.4 ± 8.8%	
45. Uridine	14.3 ± 6.9%	2.8 ± 5.2%	18.9 ± 2.8%	
46. Thymidine	23.4 ± 2.5%	1.7 ± 3.4%	21.3 ± 4.9%	
47. Cytidine	18.0 ± 1.2%	16.0 ± 1.5%	24.5 ± 10.2%	
48. Inosine	16,700 ± 2,900 nM	50,000 ± 12,700 nM	45,100 ± 38,800 nM	
49. Guanosine	27,800 ± 9,600 nM	85,100 ± 15,700 nM	98,500 ± 28,700 nM	
50. (4-Nitrobenzyl)-6-thioguanosine	15,000 ± 3,500 nM	48,500 ± 11,300 nM	40,700 ± 26,300 nM	
51. 6-Thioguanosine	44.2 ± 2.3%	27.7 ± 5.8%	44.8 ± 18.1%	
52. 6-Thiopurine riboside	61.2 ± 3.9%	33.6 ± 3.3%	41.9 ± 5.0%	
53. NECI	43.7 ± 10.3%	30.6 ± 2.3%	5,000 ± 1,150 nM	
non-xanthine adenosine antagonists				
54. CP 66713	270 nM	21 nM	29.7 ± 7.8%	(32)
55. CGS 15943	21 nM	3.3 nM	38.0 ± 14.5%	(33)
56. IQA	1,600 nM	1,400 nM	32.6 ± 10.8%	(8)
57. 9-Ethyl-N^6-cyclopentyladenine	440 nM	17,000 nM	30.4 ± 9.1%	(34)
58. EHNA	455 ± 10 nM	59.6 ± 2.8%	57.5 ± 14.3%	
59. Amiloride	11,000 nM	17,000 nM	22.0 ± 3.5%	(35)
60. Xanthine	298,000 nM	16.2 ± 2.6%	14.0 ± 7.9%	(36)
61. 1-MethylX	11,400 nM	36,200 nM	11.1 ± 1.6%	(23)
62. 3-MethylX	35,000 nM	38.0 ± 0.9%	18.1 ± 6.7%	(37)
63. 7-MethylX	52.3 ± 7.9%	37.7 ± 4.9%	16.4 ± 9.6%	
64. 9-MethylX	26.6 ± 3.2%	16.1 ± 1.9%	22.8 ± 9.5%	
65. 1,3-DimethylX (theophylline)	8,500 nM	25,000 nM	23.1 ± 9.5%	(23)
66. 1,7-DimethylX (paraxanthine)	30,000 nM	19,400 ± 3500 nM	15.5 ± 12.1%	(38)
67. 1,9-DimethylX	29.4 ± 1.6%	6.0 ± 6.3%	17.0 ± 7.9%	
68. 3,7-DimethylX (theobromine)	83,400 nM	187,000 nM	19.9 ± 7.1%	(23)
69. 3,9-DimethylX	19.7 ± 7.9%	4.2 ± 5.9%	19.0 ± 6.8%	
70. 1-Methyl-3-ButylX	7,000 nM	16,000 nM	30.1 ± 12.4%	(23)
71. 1,3-DibutylX	500 nM	2,930 ± 700 nM	143,000 ± 29,000 nM	(39)
72. 1,3-DihexylX	1,260 ± 90 nM	14.3 ± 3.0% (10 μM)	9.2 ± 6.5% (10 μM)	
73. 1,3-DibenzylX	2,000 nM	3.61 ± 0.94% (10 μM)	20.3 ± 8.5% (10 μM)	(39)

Compound	A_1 affinity[a]	A_{2a} affinity[b]	A_3 affinity[c]	Reference
74. 1,3,7-TrimethylX (caffeine)	29,000 nM	48,000 nM	30.1 ± 12.4%	(23)
75. 1,3,9-TrimethylX (isoC)	>1,000,000 nM	14.4 ± 5.7%	13.2 ± 12.4%	(40)
76. 2-Thio-3-propylX	26,100 ± 1,500 nM	32,500 ± 4,800 nM	27.7 ± 11.3%	
7-substituted alkylxanthines				
77. 7-BenzylT	6,000 nM	46,000	29.7 ± 0.2%	(41)
78. 7-β-HydroxyethylT	105,000 nM	17,400 ± 900	21.1 ± 13.3%	(39)
79. T-7-Riboside	27,000 ± 3,200 nM	n.t.	89,400 ± 13,400 nM	
80. 1,3-DipropylX-7-riboside	15,900 ± 1,800 nM	32.0 ± 1.1%	81,200 ± 10,700 nM	
81. 1,3-DibutylX-7-riboside	4,190 ± 1030 nM	19,500 ± 4,200 nM	6,030 ± 2,320 nM	
8-substituted alkylxanthines				
82. 8-PhenylT	86 nM	850 nM	12.0 ± 6.0%	(23)
83. 8-CyclopentylT	11 nM	1,400 nM	38.7 ± 2.5%	(23)
84. 8-Cyclopentyl-1-propylX	226 ± 37 nM	48,700 ± 5,000 nM	22.6 ± 7.7%	
85. 8-Cyctopentyl-1,3-dipropylX	0.46 nM	340 nM	18.7 ± 2.9% (10 μM)	(42)
86. 8-CyclohexylC	28,000 nM	10,400 ± 2,600 nM	35.2 ± 1.8%	(37)
87. 8-ChloroT	30.2 ± 6.7%	24.7 ± 3.9%	16.8 ± 9.5%	
88. XAC	1.2 nM	63 nM	7.1 ± 0.9%	(43,22)
89. 8-(3-Chlorostryryl)C (CSC)	28,200 nM	54 nM	4.2 ± 5.1% (10 μM)	(46)
90. 8-Sulfophenyl-1,3-dipropylX	140 nM	790 nM	21.9 ± 6.2%	(47)

[a] Displacement of [^{3}H]PIA (or [^{3}H]CHA) binding from rat brain membranes.

[b] Displacement of [^{3}H]CGS 21680 (or [^{3}H]NECA in the presence of 50 nM CPA) from rat striatal membranes.

[c] Displacement of [^{125}I]APNEA binding from membranes of CHO cells stably transfected with the rat A_3-cDNA.

[d] The abbreviations used are: ADAC, N^6-[4-[[[4-[[[(2-aminoethyl)amino]carbonyl]methyl]anilino]carbonyl]methyl]phenyl]adenosine; DPMA, N^6-[2-(3,5-dimethyoxyphenyl)-2-(2-methylphenyl)ethyl]adenosine; IQA, imidazo[4,5-*c*]quinolin-4-amine; EHNA, *erythro*-9-(2-hydroxy-3-nonyl)adenine; X, xanthine; T, theophylline; C, caffeine; n.t., not tested.

[*] AMP displayed an extremely high slope factor (3.62 ± 0.39 μM) in A_1 displacement. The apparent K_i, was 47.5 ± 6.5 μM.